Iranian Journal of Pharmaceutical Sciences
2023: 19 (4): 279- 292
https://journals.sbmu.ac.ir/IJPS

Original Article

Solubility determination and thermodynamic modeling of deferiprone in the binary aqueous mixtures of 2-propanol from 293.15 to 313.15 K

Homa Rezaei[a,b], Elaheh Rahimpour[b,c*], Fleming Martinez[d], Abolghasem Jouyban[b,e]

[a]Student Research Committee, Faculty of Pharmacy, Tabriz University of Medical Sciences, Tabriz, Iran, [b]Pharmaceutical Analysis Research Center and Faculty of Pharmacy, Tabriz University of Medical Sciences, Tabriz, Iran, [c]Infectious and Tropical Diseases Research Center, Tabriz University of Medical Sciences, Tabriz, Iran, [d]Grupo de Investigaciones Farmacéutico-Fisicoquímicas, Departamento de Farmacia, Universidad Nacional de Colombia, Sede Bogotá, Cra. 30 No. 45-03, Bogotá D. C., Colombia, [e]Faculty of Pharmacy, Near East University, Nicosia, North Cyprus, Turkey.

Abstract

In the current work, solid-liquid equilibrium measurements and data correlations of deferiprone in 2-propanol + water were carried out. Mathematical models (van't Hoff, λh, modified Wilson, Jouyban-Acree, and Jouyban-Acree-van't Hoff) were utilized for correlating the experimental solubility data, and their accuracy was computed by mean relative deviation of the back-calculated data. Furthermore, the apparent thermodynamic parameters of the deferiprone dissolution process were computed by the Gibbs and van't Hoff equations to analyze the solubility behavior in the investigated mixtures. The results from the analysis and testing of deferiprone solubility data were expected to assist crystallization processes, industrial production, and formulation research.

Keywords: Binary solvent mixtures; Deferiprone; Thermodynamics; Cosolvency models.

1. Introduction

Thalassemia is a frequently common genetic disorder involving absent or impaired formation of one or more hemoglobin chains [1-3]. Patients who are diagnosed with thalassemia are susceptible to both thromboembolism and iron overload, as orderly blood transfusions are required [4]. Exposure to excess amounts of iron leads to platelet hyper-activation and the generation of oxygen-free radicals that precipitate multiple complications [5, 6]. Deferiprone (3-hydroxy-1, 2-dimethylpyridin-4(1H)-one, **Figure 1** is an iron chelator that has been developed for alleviating platelet hyper-activation in thalassemia over the past 20 years. Additionally, deferiprone is supposed to exhibit antioxidant activity, preventing oxidative stress and cellular, subcellular, bimolecular, and tissue damage from copper and iron-induced free radical formation [7].

Corresponding Author: Elaheh Rahimpour, *Pharmaceutical Analysis Research Center and Faculty of Pharmacy, Tabriz University of Medical Sciences, Tabriz, Iran*. E-mails: rahimpour_e@yahoo.com.

Cite this article as: Rezaei H, Rahimpour E, Martinez F, Jouyban A, *Solubility determination and thermodynamic modeling of deferiprone in the binary aqueous mixtures of 2-propanol from 293.15 to 313.15 K*, Iran. J. Pharm. Sci., 2023, 19 (4): 279- 292.

DOI: https://doi.org/10.22037/ijps.v19i4.43600

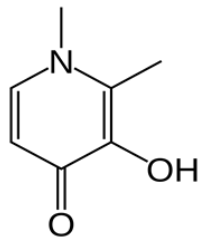

Figure 1. Molecular structure of deferiprone.

Deferiprone is orally available in the pharmaceutical market as tablets (Ferriprox®, Apotex®). Recently, pharmaceutical professionals have been trying to develop a liquid formulation for young children and those experiencing difficulties swallowing tablets [8]. Enhancement of drug solubility and, consequently, its oral bioavailability has always remained one of the major challenges during the process of drug development, specifically when the drug is supposed to be delivered via the oral route.

Over the past 15 years, the importance of solubility has been revealed to the pharmaceutical industry, and multiple strategies have been developed to either enhance candidate drugability or dominate poor solubility profiles employing solubilization techniques [9-11]. These methods include modifying the drug's structure to enhance solubility, applying *in silico* approaches during the structural design process for solubility risk prediction, screening solubility to examine potential issues early, and developing formulations to enhance solubility and dissolution rate [12]. Therefore, the development of strategies and methodologies that have the potential ability to bridge the differences existing between drug discovery and development is of utmost importance. Additionally, knowledge of solubility yields crucial information for the intermolecular and drug structure [13]. Among various approaches that the pharmaceutical industry has recognized for enhancing drug solubility, adding a less polar solvent to water, known as cosolvency, is a frequently used method. By adopting this methodology, pharmaceutical experts can augment the solubility of hydrophobic medications and diminish the solubility of hydrophilic and/or ionized medications [14]. In the literature, the solubility of deferiprone in mixtures of ethylene glycol, propylene glycol, polyethylene glycol 400 [14], ethanol, N-methyl-2-pyrrolidone [15], and some mono-solvents such as ethyl acetate, chloroform, acetonitrile, 1,4-dioxane, and dichloromethane [16] has been investigated. The objectives of this study were to compile a comprehensive solubility database for deferiprone in cosolvency systems. These objectives included (1) determining the solubility and density of deferiprone saturated solutions in mixtures of 2-propanol and water at temperatures ranging from 293.2 to 313.2 K, (2) establishing correlations between the gathered data and established cosolvency models, and (3) calculating the apparent thermodynamic parameters for the dissolution process of deferiprone, along with the preferential solvation parameters in the investigated mixtures.

In brief, this research focuses on the pharmaceutical aspects of solubility and thermodynamic modeling in determining the solubility of deferiprone in 2-propanol and water. The importance of this study lies in its contribution to pharmaceutical sciences, specifically compared to other solubility media. By investigating the solubility of deferiprone in these solvent mixtures, valuable insights can be gained regarding their suitability in drug formulation and delivery. Even if previous studies have investigated deferiprone's solubility, our study contributes to the existing

literature by providing new data points for deferiprone solubility in the aqueous mixture of 2-propanol. It can help researchers make further comparisons, draw more comprehensive conclusions, and potentially contribute to developing more accurate predictive models.

Understanding the solubility of a drug in different media is crucial for optimizing drug formulation and ensuring drug efficacy. Additionally, using solubility and thermodynamic modeling allows for a deeper understanding of the physicochemical properties of drugs, aiding in developing more efficient and effective pharmaceutical formulations. This research ultimately contributes to drug design and formulation advancements, thus benefiting patients by improving drug delivery and therapeutic outcomes in pharmaceutical sciences.

2. Materials and Methods

2.1. Materials

2-Propanol used for solvent mixture preparation was the analytical grade and ethanol and lab-made distilled water were employed in the saturated solutions' dilution process. The experimental reagents' purification was greater than 0.990; therefore, no further purification was required. Purity, source, analysis method, and other detailed specifications of the materials used during the process are listed in **Table 1**.

2.2. Measurement of deferiprone solubility

The shake-flask method was used to determine the solid-liquid equilibrium of deferiprone within mixed solvents (2-propanol + water), and data was assessed using a spectrophotometry method. The general procedure can be described as follows. Eleven dry glass vials were prepared to be filled with water and 2-propanol as a cosolvent with a mass ratio of 0.0 - 1.0.

Then, excess deferiprone was added to the prepared solvent mixtures, transferred to an incubator (Kimia Idea Pardaz Azerbaijan, Tabriz, Iran), and stirred for 48 hours on a shaker (Behdad, Tehran, Iran). After establishing equilibrium, the supernatant was centrifuged, and an appropriate liquid was gently removed from the saturated solution and transferred to another tube to be appropriately diluted with the corresponding solvent mixture (ethanol: water, 30:70 % v/v). Diluted solutions were analyzed using a UV-Vis spectrophotometer (Cecil BioAquarius CE 7250, UK) at 273.5 nm. The calibration curve was plotted from deferiprone standard solutions with concentrations in 1.0×10^{-5} - 1.5×10^{-4} mol·L^{-1}. The calibration plot was found to be linear with a R^2 = 0.9996. The densities of the saturated solutions were determined using a 5 mL pycnometer with a precision of 0.001 g·cm^{-3}.

Table 1: Information of substances used in the work ahead.

Chemical Name	CAS Number	Molecular formula	Molar mass (g·mol^{-1})	Source	Purity (percentage)	Analysis method
Deferiprone	30652-11-0	$C_7H_9NO_2$	139.15	Arasto Pharmaceutical Chemicals Inc	≥ 99.7 %	HPLC[a]
2-Propanol	67-63-0	C_3H_8O	60.10	Merck	≥ 99.8 %	GC[b]
Distilled deionized water	7732-18-5	H_2O	18.02	Shahid Ghazi Pharmaceutical Co.	≥ 99.9 %	GC[b]
Ethanol	64-17-5	C_2H_5OH	46.07	Jahan Alcohol Teb	≥ 93.5 %	GC[b]

[a] High-performance liquid chromatography
[b] Gas chromatography

2.3. X-ray powder diffraction (XRD) analysis

The crystallinity of deferiprone (in its raw form and any residual amount present in 2-propanol and water) was analyzed using XRD on a PHILIPS PW1730 instrument. The XRD data were obtained by measuring the diffraction pattern from 10° to 40° (2θ) at a current of 30 mA and a voltage of 40 kV in ambient conditions.

2.4. Computation

The experimental solubility data were compared with different computational models (van't Hoff, *λh*, modified Wilson, Jouyban-Acree, and Jouyban-Acree-van't Hoff) that effectively describe the connections between temperature, solubility, and initial solvent composition. The specific information regarding each model is presented in the subsequent sections. In each section, data can be calculated backward using Eq. (1) to assess the accuracy of each model, which is determined through the mean relative deviation (MRD%) calculated using Eq. (1).

$$MRD\% = \frac{100}{N}\sum\left(\frac{|Calculated\ Value - Observed\ Value|}{Observed\ Value}\right) \quad (1)$$

N demonstrates the number of data points.

2.4.1. van't Hoff equation

Eq. (2) illustrates the van't Hoff equation, a two-parameter empirical equation used to describe the trend of mole fraction solubility at different temperatures [17]:

$$lnx\_ = A + B/T \quad (2)$$

Where *A* and *B* are defined as the model parameters.

2.4.2. λh Equation

The λh equation, introduced by Buchowski and co-workers [18], investigates the connection between solubility and temperature. This equation, which consists of two parameters (λ and h), specifically describes the solvent activity along a saturation line and the solubility of solids with hydrogen bonding. It is expressed as follows:

$$\ln\left[1+\lambda\frac{1-x}{x}\right] = \lambda h\left(\frac{1}{T}-\frac{1}{T_m}\right) \quad (3)$$

T and T_m are the solution and solute melting temperatures (545.2 K for deferiprone), respectively. λ and h represent the model coefficients.

2.4.3. The Jouyban-Acree model

The Jouyban-Acree model, a linear mathematical model, is used to explain the relationship between solubility temperature and solvent composition. The equation for this model is provided in Eq. (4). [19]:

$$\ln x_{m.T} = w_1 \ln x_{1.T} + w_2 \ln x_{2.T} + \frac{w_1.w_2}{T}\sum_{i=0}^{2} J_i.(w_1 - w_2)^i \quad (4)$$

in which $x_{1,T}$ and $x_{2,T}$ are the solubility values in mono-solvents at a temperature of T, w_1 and w_2 are the mass ratios of solvents 1 and 2 in the absence of solute, and J_i terms are the model parameters achieved by linear regression of

$(\ln x_{m.T} - w_1 \ln x_{1.T} - w_2 \ln x_{2.T})$ against $\frac{w_1.w_2}{T}$, $\frac{w_1.w_2(w_1-w_2)}{T}$, and $\frac{w_1.w_2(w_1-w_2)^2}{T}$.

2.4.4. The Jouyban-Acree-van't Hoff model

Combining the van't Hoff equation and the Jouyban-Acree model provides an accurate model for predicting solubility data in cosolvency systems [19]. This model, known as the Jouyban-Acree-va Hoff model, is expressed as follows:

$$\ln x_{m.T} = w_1\left(A_1 + \frac{B_1}{T}\right) + w_2\left(A_2 + \frac{B_2}{T}\right) + \frac{w_1.w_2}{T}\sum_{i=0}^{2} J_i.(w_1 - w_2)^i \quad (5)$$

A_1, B_1, A_2, and B_2 are the van't Hoff model's constants obtained by plotting ln $x_{m,T}$ against $1/T$ in the mono-solvents at various temperatures. J_i terms are computed using linear regression of

$$\left(\ln x_{m.T} - w_1\left(A_1 + \frac{B_1}{T}\right) - w_2\left(A_2 + \frac{B_2}{T}\right)\right) \; vs \; \frac{w_1.w_2}{T}.\ \frac{w_1.w_2(w_1-w_2)}{T}.\ and\ \frac{w_1.w_2(w_1-w_2)^2}{T}.$$

2.4.5. The modified Wilson model

modified Wilson equation is written as follows:

$$-lnx_m = 1 - \frac{w_1[1+lnx_1]}{w_1+w_2\lambda_{12}} - \frac{w_2[1+lnx_2]}{w_1\lambda_{21}+w_2} \quad (6)$$

By performing a straightforward non-linear analysis using λ_{12} and λ_{21} as the parameters in the equation, the values of these parameters can be determined [20].

2.5. Thermodynamic parameters

The mixing thermodynamic functions, including the apparent standard dissolution Gibbs energy ($\Delta G°$), standard dissolution enthalpy ($\Delta H°$), and standard dissolution entropy change ($\Delta S°$), were used to describe the dissolution behavior of deferiprone. The apparent thermodynamic parameters were computed using the Gibbs and modified van't Hoff equations. The following equation manifests the latter:

$$\frac{\partial \ln x}{\partial\left(\frac{1}{T} - \frac{1}{T_m}\right)_p} = -\frac{\Delta H^\circ}{R} \quad (7)$$

The variable *x* represents the contribution of the solute to solubility, expressed in mole fraction units. *R* is the ideal gas constant, and *T* is the absolute temperature in Kelvin. T_{hm} denotes the mean harmonic temperature, computed based on the equation provided

$$T_{hm} = n / \sum_{i=1}^{n}(1/T)$$

(*n* is the number of studied temperatures) [21]. The slope and intercept of the graph of ln x versus $1/T - 1/T_{hm}$ are utilized to determine ΔH° and ΔG° for saturated mixtures, respectively. ΔS° values are also calculated using the Gibbs equation."

For binary solvent mixtures, the entropy (ζ_{TS}) and enthalpy (ζ_H) can be used to compare the relative contributions, and they are depicted as follows [22]:

$$\zeta_H = \frac{|\Delta H^\circ|}{(|\Delta H^\circ| + |T\Delta S^\circ|)} \quad (8)$$

$$\zeta_{TS} = \frac{|T\Delta S^\circ|}{(|\Delta H^\circ| + |T\Delta S^\circ|)} \quad (9)$$

3. Results and Discussion

3.1. Solubility profile of deferiprone and data modeling

The solubility of deferiprone in aqueous binary mixtures containing varying amounts of

2-propanol and the corresponding temperatures are presented in **Table 2.** Since as the temperature enhances, the molecular motion rate and the interval between solvent molecules become greater, the solubility of deferiprone was expected to increase with the increase in temperature, and this trend was well observed in this Table at different temperatures.

Table 2: Experimental mole fraction solubility ($x_{m,T}$) and molar solubility ($C_{m,T}$) values as the mean of three experiments (± standard deviation) measured for deferiprone in the binary mixtures of 2-propanol and water at different temperatures.

w_1[a]	293.2 K	298.2 K	303.2 K	308.2 K	313.2 K
			$x_{m,T}$		
0.00	1.58 (±0.07) × 10^{-3}	1.81 (±0.14) × 10^{-3}	2.21 (±0.17) × 10^{-3}	2.78 (±0.31) × 10^{-3}	3.21 (±0.17) × 10^{-3}
0.10	2.14 (±0.09) × 10^{-3}	2.46 (±0.04) × 10^{-3}	3.04 (±0.35) × 10^{-3}	3.39 (±0.42) × 10^{-3}	4.41 (±0.41) × 10^{-3}
0.20	2.65 (±0.08) × 10^{-3}	3.18 (±0.08) × 10^{-3}	3.81 (±0.00) × 10^{-3}	4.31 (±0.02) × 10^{-3}	5.58 (±0.30) × 10^{-3}
0.30	3.09 (±0.20) × 10^{-3}	4.07 (±0.11) × 10^{-3}	4.65 (±0.04) × 10^{-3}	5.35 (±0.04) × 10^{-3}	6.83 (±0.38) × 10^{-3}
0.40	3.27 (±0.05) × 10^{-3}	4.30 (±0.06) × 10^{-3}	5.19 (±0.34) × 10^{-3}	5.91 (±0.12) × 10^{-3}	7.42 (±0.07) × 10^{-2}
0.50	3.31 (±0.44) × 10^{-3}	4.36 (±0.12) × 10^{-3}	5.49 (±0.42) × 10^{-3}	6.37 (±0.26) × 10^{-3}	7.94 (±0.42) × 10^{-3}
0.60	3.48 (±0.08) × 10^{-3}	4.38 (±0.03) × 10^{-3}	5.26 (±0.03) × 10^{-3}	6.49 (±1.36) × 10^{-3}	8.04 (±0.98) × 10^{-3}
0.70	3.38 (±0.00) × 10^{-3}	4.03 (±0.07) × 10^{-3}	4.86 (±0.17) × 10^{-3}	5.68 (±0.25) × 10^{-3}	7.34 (±0.21) × 10^{-3}
0.80	3.04 (±0.21) × 10^{-3}	3.46 (±0.16) × 10^{-3}	4.01 (±0.37) × 10^{-3}	4.61 (±0.49) × 10^{-3}	6.08 (±0.08) × 10^{-3}
0.90	2.53 (±0.13) × 10^{-3}	2.69 (±0.11) × 10^{-3}	3.16 (±0.06) × 10^{-3}	3.66 (±0.11) × 10^{-3}	4.61 (±0.15) × 10^{-3}
1.00	9.35 (±0.24) × 10^{-4}	1.05 (±0.05) × 10^{-3}	1.32 (±0.05) × 10^{-3}	1.67 (±0.22) × 10^{-3}	2.03 (±0.11) × 10^{-3}
			$C_{m,T}$		
0.00	8.69 (±0.09) × 10^{-2}	9.89 (±0.07) × 10^{-2}	1.21 (±0.05) × 10^{-1}	1.51 (±0.17) × 10^{-1}	1.74 (±0.09) × 10^{-1}
0.10	1.08 (±0.17) × 10^{-1}	1.23 (±0.02) × 10^{-1}	1.51 (±0.05) × 10^{-1}	1.68 (±0.09) × 10^{-1}	2.18 (±0.19) × 10^{-1}
0.20	1.21 (±0.01) × 10^{-1}	1.44 (±0.04) × 10^{-1}	1.73 (±0.04) × 10^{-1}	1.94 (±0.05) × 10^{-1}	2.50 (±0.13) × 10^{-1}
0.30	1.28 (±0.01) × 10^{-1}	1.66 (±0.04) × 10^{-1}	1.89 (±0.08) × 10^{-1}	2.17 (±0.18) × 10^{-1}	2.74 (±0.15) × 10^{-1}
0.40	1.21 (±0.12) × 10^{-1}	1.57 (±0.02) × 10^{-1}	1.88 (±0.02) × 10^{-1}	2.13 (±0.04) × 10^{-1}	2.66 (±0.26) × 10^{-1}
0.50	1.07 (±0.13) × 10^{-1}	1.40 (±0.04) × 10^{-1}	1.76 (±0.02) × 10^{-1}	2.03 (±0.08) × 10^{-1}	2.51 (±0.13) × 10^{-1}
0.60	9.67 (±0.08) × 10^{-2}	1.21 (±0.08) × 10^{-1}	1.44 (±0.02) × 10^{-1}	1.77 (±0.36) × 10^{-1}	2.18 (±0.26) × 10^{-1}
0.70	8.19 (±0.39) × 10^{-2}	9.71 (±0.36) × 10^{-2}	1.16 (±0.01) × 10^{-1}	1.35 (±0.06) × 10^{-1}	1.73 (±0.50) × 10^{-1}
0.80	6.19 (±0.07) × 10^{-2}	6.99 (±0.03) × 10^{-2}	8.09 (±0.44) × 10^{-2}	9.25 (±0.10) × 10^{-2}	1.21 (±0.16) × 10^{-2}
0.90	4.20 (±0.10) × 10^{-2}	4.45 (±0.18) × 10^{-2}	5.21 (±0.22) × 10^{-2}	6.00 (±0.18) × 10^{-2}	7.51 (±0.24) × 10^{-2}
1.00	1.22 (±0.06) × 10^{-2}	1.37 (±0.06) × 10^{-2}	1.71 (±0.03) × 10^{-2}	2.16 (±0.22) × 10^{-2}	2.61 (±0.14) × 10^{-2}

[a] w_1 is the mass fraction of 2-propanol in the 2-propanol and water mixtures without deferiprone.

Also, it showed a positive relationship with a 2-propanol mass fraction increasing up to 0.6. Several factors can explain the maximum solubility of deferiprone in 2-propanol-rich mixtures. These include the solvent-solute interactions facilitated by the polar aprotic nature of 2-propanol, the intermediate polarity of 2-propanol that enhances solubility for compounds like deferiprone, and the potential similarity in solubility parameters between deferiprone and 2-propanol However, the maximum solubility of deferiprone in 2-propanol at a mass fraction of 0.6 may be attributed to non-ideal solution behavior.

This can occur when the solvent mixture deviates from ideal behavior due to molecular interactions and solute-solvent association. Non-ideal behavior can affect the solubility, resulting in a maximum at a specific composition. For investigation of data accuracy, the measured datum for deferiprone in neat water (9.89×10^{-2} mol·L^{-1}) was compared with database one (1.15×10^{-1} mol·L^{-1} [23] at 298.2 K, and a tiny difference demonstrated the obtained data possess good acceptance for the report. Moreover, **Figure 2** depicts the deferiprone solubility expressed in mol·L–1 at all temperatures.

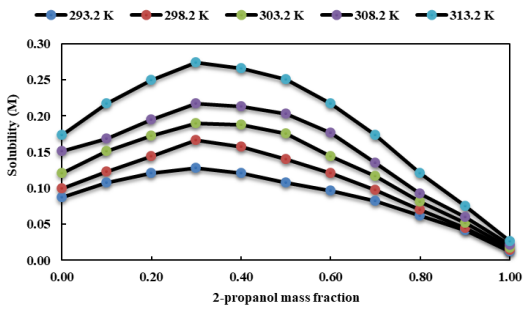

Figure 2. Molarity solubility of deferiprone in the mixtures of 2-propanol and water at different temperatures. From bottom to top: 293.2 K, 298.2 K, 303.2 K, 308.2 K, 313.2 K.

Using an XRD instrument at normal temperature and pressure, the XRD data of deferiprone residues in single solvents were obtained, and their patterns are presented in **Figure 3.** This analysis helps determine whether solid deferiprone forms solvated compounds or polymorphs in saturated solutions. The results indicate that no new characteristic peaks appeared, implying that the crystallinity of deferiprone did not change and did not undergo a polymorphic transformation during the dissolution process.

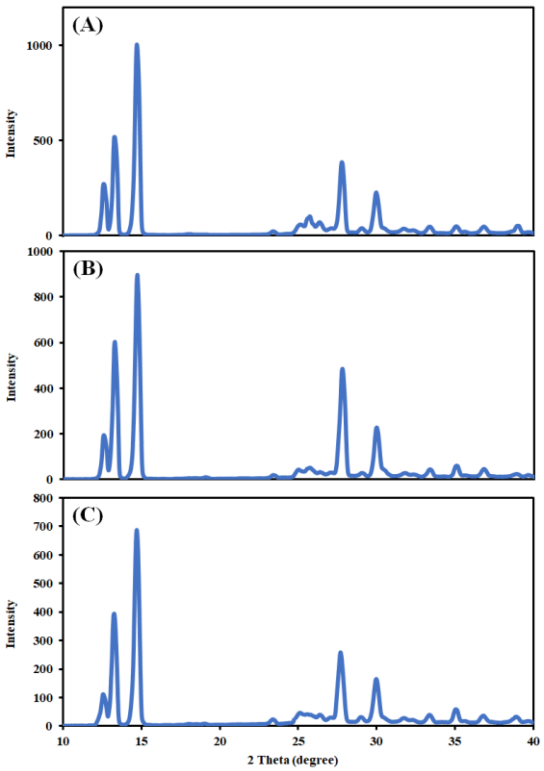

Figure 3. XRD pattern of raw deferiprone (A) and equilibrated deferiprone in water (B) and 2-propanol (C).

To determine the polarity of deferiprone, **Figure 4** displays the mole fraction solubility as a function of the Hildebrand solubility parameter for the aqueous 2-propanol mixtures at a temperature of 298.2 K (δ_{1+2}), which is a commonly employed polarity index. The

maximum solubility of drugs is typically observed when the polarities of solute and solvents coincide. Thus, the Hildebrand solubility parameter of deferiprone is expected to be around 32 $MPa^{1/2}$. However, this value differs from the one calculated using the group contribution method proposed by Fedors (**Table 3**), which is 27.8 $MPa^{1/2}$. [24, 25].

Table 3: Application of the Fedors method to estimate internal energy, molar volume, and Hildebrand solubility parameter of deferiprone.

Group	Group number	$\Delta U°$ (kJ·mol^{-1})	$V°$ (cm^3·mol^{-1})
–CH_3	2	9.42	67.0
–CH=	2	8.62	27.0
>C=	2	8.62	–11.0
6-atoms ring closure	1	1.05	16.0
Conjugation in ring	2	3.34	–4.4
–OH	1	29.8	10.0
–CO–	1	17.4	10.8
–N<	1	4.2	–9.0
		$\Sigma\ \Delta U° = 82.45$	$\Sigma\ V = 106.4$
		$\delta_3 = (82{,}450/106.4)^{1/2} = 27.84\ MPa^{1/2}$	

The $U°$ parameter typically represents the potential energy of a system, while $V°$ represents the molar volume.

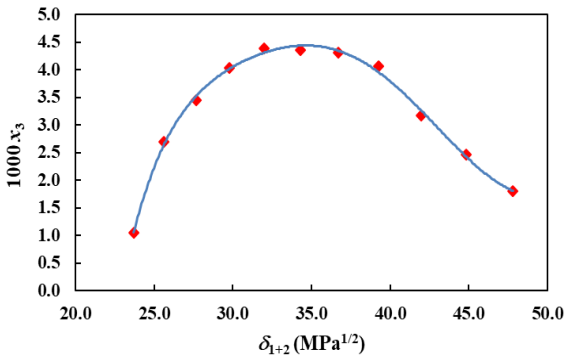

Figure 4. Mole fraction solubility of deferiprone in the mixtures of 2-propanol and water at 298.2 K as a function of the Hildebrand solubility parameter of the mixtures in the absence of deferiprone. (x_3 mole fraction solubility of deferiprone and δ_{1+2} is Hildebrand solubility parameter of the aqueous 2-propanol mixtures).

Owing to this difference between both estimation methods, it is concluded that polarity is not the only thing involved in drug solubilities.

In the next part, the Jouyban-Acree, the λh, the van't Hoff, the modified Wilson, and Jouyban-Acree-van't Hoff models were chosen to fit the experimental solubility data, and the acquired results were listed in **Tables 4-7**.

Table 4: The van't Hoff model parameters and the corresponding *MRD*% for deferiprone in the binary mixtures of 2-propanol and water.

w_1	*A*	*B*	*MRD*%
0.00	5.084	-3389.662	2.2
0.10	4.879	-3239.885	3.0
0.20	5.279	-3290.115	2.0
0.30	5.901	-3416.730	3.0
0.40	6.579	-3597.779	2.7
0.50	7.672	-3915.277	2.4
0.60	7.291	-3797.457	0.9
0.70	6.141	-3474.103	2.2
0.80	4.618	-3063.825	3.9
0.90	3.376	-2759.039	4.3
1.00	5.578	-3693.994	3.0
Overall			2.7

A and *B* are van't Hoff model parameters.

Table 5: The λh equation constants and the *MRD*% for the back-calculated solubility of deferiprone solubility in the binary mixture of 2-propanol and water.

w_1	λ	*h*	*MRD*%
0.00	0.507	31.075	4.3
0.10	0.509	40.080	5.3
0.20	0.512	51.162	4.6
0.30	0.514	64.084	4.0
0.40	0.516	72.503	2.6
0.50	0.518	82.440	2.3
0.60	0.518	82.051	4.0
0.70	0.516	69.900	5.2
0.80	0.512	52.803	6.4
0.90	0.509	37.510	6.3
1.00	0.504	20.656	6.0
Overall			4.6

λ and *h* are λh equation constants.

Table 6: The λh equation constants and the *MRD*% for the back-calculated solubility of deferiprone solubility in the binary mixture of 2-propanol and water.

	Jouyban-Acree		Jouyban-Acree-van't Hoff	
2-Propanol + water	J_0	1330.446	A_1	5.578
--	J_1	650.536	B_1	-3693.994
--	J_2	813.169	A_2	5.084
--	--	--	B_2	-3389.662
--	--	--	J_0	1330.832
--	--	--	J_1	650.335
--	--	--	J_2	814.133
MRD%	5.0		5.1	

J_i is Jouyban-Acree model parameters. J_i A_i and B_i are Jouyban-Acree-van't Hoff model parameters.

Table 7: The modified Wilson model parameters at the investigated temperatures and the *MRD*% for back-calculated deferiprone solubility in the binary mixtures of 2-propanol and water.

T (K)	λ_{12}	λ_{21}	*MRD*%
293.2	3.068	0.728	7.4
298.2	2.595	0.944	5.8
303.2	2.503	0.986	4.4
308.2	2.578	0.918	2.7
313.2	2.588	1.019	3.7
Overall			4.8

λ_{ij} are modified Wilson model parameters

As can be seen, the van't Hoff model processed the most accurate results in comparison with the other four models (*MRD*%= 2.7%). The *MDR%* values of the employed mathematical models were in the following order: the van't Hoff (2.7%) < the λh (4.6%) < the modified Wilson model (4.8%) < the Jouyban-Acree (5.0%) < Jouyban-Acree-van't Hoff (5.1%). The low deviation observed for the van't Hoff model (2.7%) compared to other models is likely due to (i) Applicability of the model to dilute solutions: The van't Hoff model is most accurate for dilute solutions, where the solute concentration is low. In such cases, the interactions between solute molecules become less prevalent, and the assumption of negligible interactions in the model becomes more valid. As a result, the van't Hoff model can give good approximations for dilute solutions, leading to low deviations and (ii) limited temperature range: The van't Hoff model assumes that the enthalpy change with temperature is constant over the temperature range studied. If the temperature range used for comparing models is relatively small or the behavior of the solute-solvent system is not highly temperature-dependent, the van't Hoff model can provide accurate predictions with a low deviation. Furthermore, in the above comparison, the Jouyban-Acree and Jouyban-Acree-van't Hoff models had high deviation. However, they were developed considering temperature and cosolvent mass fraction, and data training was conducted in one step. This approach provides a single model for all correlated data, a major advantage over other models. Moreover, the Jouyban-Acree-van't model was a semi-predictive model., The model was trained using a minimal number of data points to assess its predictive capability, specifically the solubility values in the pure solvents at both high and low temperatures, as well as in 2-propanol concentrations of 0.3, 0.5, and 0.7 at a temperature of 298.2 K. The trained model was then employed to predict the remaining data. The *MRD*% for the predicted data at temperatures of 293.2, 298.2, 303.2, 308.2, and 313.2 K were 9.9%, 7.3%, 5.0%, 5.5%, and 8.0%, respectively.

Additionally, the densities (g/cm³) of deferiprone-saturated solutions in binary aqueous mixtures of 2-propanol at varying temperatures were measured and provided in **Table 8**. These data were also fitted to the Jouyban-Acree model, and the resulting trained model was:

$$\ln\rho_{m.T} = w_1 \ln\rho_{1.T} + w_2 \ln\rho_{2.T} + 27.835 \frac{w_1 . w_2}{T} - 9.298 \frac{w_1 . w_2 (w_1 - w_2)}{T} + 16.374 \frac{w_1 . w_2 (w_1 - w_2)^2}{T} \quad 10)$$

The very low *MRD*% of 0.3% for the back-calculated data indicates the exceptional capacity of the employed model for predicting densities at different temperatures.

3.2. Computation of apparent thermodynamic properties

Table 9 presents the obtained values for apparent thermodynamic parameters and specific contributions to the Gibbs energy for the dissolution of deferiprone. The experimental results revealed that the $\Delta S°$ values for the dissolution process of deferiprone in pure solvents and all solvent mixtures were positive, indicating that an increase in entropy accompanied the process. The $\Delta H°$ values were also positive, indicating that the deferiprone dissolution process was endothermic, meaning that it required an input of energy. The observed endothermic circumstances could be attributed to the stronger intermolecular interactions between solvent molecules. During the dissolution process of deferiprone, new bonds formed between deferiprone and solvent molecules, while the existing bonds between solvent molecules were broken. It led to an overall increase in free energy, as the energy required to form new bonds was insufficient to offset the energy required to break the existing bonds. The $\Delta G°$ values for the dissolution process ranged from 13.20 to 16.66 kJ·mol^{-1}, with the lowest value observed at w_1 = 0.6, corresponding to the solvent mixture with the highest solubility of deferiprone."

Table 8: Measured density (g·cm^{-3}) of deferiprone saturated solutions in the binary mixtures of 2-propanol and water at different temperatures.

w_1	293.2 K	298.2 K	303.2 K	308.2 K	313.2 K
0.00	1.000 ±0.001	0.999 ±0.001	0.998 ±0.001	0.997 ±0.001	0.996 ±0.001
0.10	0.985 ±0.001	0.984 ±0.001	0.983 ±0.001	0.982 ±0.001	0.981 ±0.001
0.20	0.973 ±0.001	0.969 ±0.001	0.968 ±0.001	0.968 ±0.001	0.967 ±0.001
0.30	0.955 ±0.001	0.952 ±0.001	0.951 ±0.001	0.949 ±0.001	0.946 ±0.001
0.40	0.935 ±0.001	0.930 ±0.001	0.928 ±0.001	0.928 ±0.001	0.927 ±0.001
0.50	0.913 ±0.001	0.907 ±0.001	0.906 ±0.001	0.904 ±0.001	0.903 ±0.001
0.60	0.874 ±0.001	0.869 ±0.001	0.867 ±0.001	0.866 ±0.001	0.865 ±0.001
0.70	0.864 ±0.001	0.860 ±0.001	0.857 ±0.001	0.856 ±0.001	0.853 ±0.001
0.80	0.840 ±0.001	0.836 ±0.001	0.833 ±0.001	0.830 ±0.001	0.827 ±0.001
0.90	0.814 ±0.001	0.810 ±0.001	0.807 ±0.001	0.803 ±0.001	0.800 ±0.001
1.00	0.787 ±0.001	0.782 ±0.001	0.779 ±0.001	0.777 ±0.001	0.772 ±0.001

Table 9: Apparent thermodynamic parameters for dissolution behavior of deferiprone in the binary mixtures of 2-propanol and water at T_{hm}.

w_1	$\Delta G°$ (kJ·mol^{-1})	$\Delta H°$ (kJ·mol^{-1})	$\Delta S°$ (J·K^{-1}·mol^{-1})	$T\Delta S°$ (kJ·mol^{-1})	ζ_H	ζ_{TS}
0.00	15.37	28.23	42.43	12.86	0.687	0.313
0.10	14.64	26.88	40.37	12.23	0.687	0.313
0.20	14.06	27.37	43.94	13.32	0.673	0.327
0.30	13.54	28.40	49.04	14.86	0.657	0.343
0.40	13.34	29.87	54.55	16.53	0.644	0.356
0.50	13.22	32.60	63.94	19.38	0.627	0.373
0.60	13.20	31.55	60.54	18.34	0.632	0.368
0.70	13.41	28.87	51.00	15.45	0.651	0.349
0.80	13.84	25.49	38.45	11.65	0.686	0.314
0.90	14.43	22.98	28.20	8.55	0.729	0.271
1.00	16.66	30.81	46.70	14.15	0.685	0.315

$\Delta G°$: Gibbs free energy, $\Delta H°$: Enthalpy, $\Delta S°$: Entropy, the relative contributions entropy (ζ_{TS}) and enthalpy (ζ_H) in Gibbs free energy.

Furthermore, the enthalpy-entropy compensation plot depicted in **Figure 5** revealed a non-linear trend for the deferiprone dissolution process. For solvent compositions with $0.0 \leq w_1 \leq 0.1$, the driving force for the transfer of deferiprone was enthalpy, while for other mixtures, the driving force was entropy.

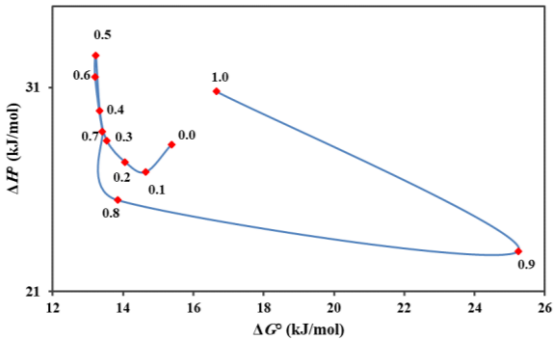

Figure 5. Enthalpy-entropy compensation plot for deferiprone in the mixtures of 2-propanol and water at 303.0 K. The points represent the mass fraction of 2-propanol in 2-propanol and water mixtures without deferiprone.

The respective preferential solvation analysis at 298.2 K was performed based on the inverse Kirkwood-Buff integrals (IKBI) mentioned in the database to inquire about the molecular mechanism of cosolvency involved in deferiprone dissolution [26]. Mathematical procedures and general thermodynamic quantities required in calculations can be found in our previous paper [27]. Because Gibbs' energy of transfer of deferiprone from pure to all aqueous 2-propanol mixtures is required for the IKBI method, **Figure 6** depicts all these values as computed from mole fraction solubilities summarized in Table 2.

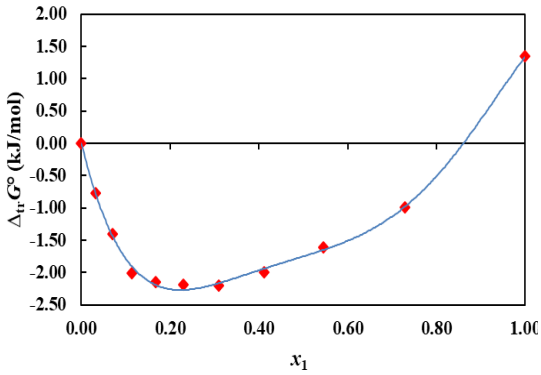

Figure 6. Gibbs energy of transfer of deferiprone from neat water ($\Delta_{tr}G°$) to all the mixtures of 2-propanol and water at 298.2 K. x_1 is mole fraction of 2-propanol in the mixtures of 2-propanol and water.

Moreover, deferiprone's molar volume is calculated here using the Fedors method, 106.4 $cm^3 \cdot mol^{-1}$ (Table 3). The correlation radius of deferiprone was computed as 0.348 nm. **Table 10** summarizes the specific thermodynamic quantities relative to the preferential solvation of deferiprone by 2-propanol in these mixtures. Graphically, **Figure 7** depicts the preferential solvation parameters of deferiprone by 2-propanol ($\delta x_{1,3}$). As observed, this drug is preferentially solvated by water (owing to the negative values of $\delta x_{1,3}$) in almost all mixture compositions.

Nevertheless, in water-rich mixtures, the negative $\delta x_{1,3}$ magnitudes are smaller than |0.01| and are a result of uncertainties propagation in IKBI calculations, but in the interval of $0.20<x_1<1.00$, the negative $\delta x_{1,3}$ magnitudes are higher than |0.01| and thus, they are attributed to real preferential solvation impacts of deferiprone by molecules of water. Preferential hydration of deferiprone in this mixture interval could be attributed to the Lewis acidic behavior of water establishing hydrogen bonding with amine or carbonyl groups of this drug.

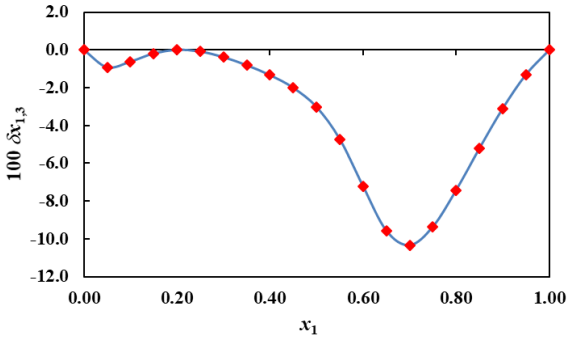

Figure 7. Preferential solvation parameters of deferiprone by 2-propanol in the mixtures of 2-propanol and water at 298.2 K. (x_1 is the mole fraction of 2-propanol in the mixtures of 2-propanol and water and $\delta x_{1,3}$ is preferential solvation parameters of deferiprone by 2-propanol).

Table 10: Some properties associated with preferential deferiprone (3) solvation in aqueous 2-propanol mixtures at 298.2 K.

x_1 [a]	D (kJ/mol)	$G_{1,3}$ (cm^3/mol)	$G_{2,3}$ (cm^3/mol)	V_{cor} (cm^3/mol)	100 $\delta x_{1,3}$
0.00	-27.93	-308.2	-105.3	602	0.00
0.05	-17.33	-228.4	-131.2	644	-0.91
0.10	-9.70	-174.2	-136.3	697	-0.61
0.15	-4.45	-137.4	-128.6	750	-0.18
0.20	-1.07	-113.0	-113.4	800	0.01
0.25	0.91	-97.3	-94.2	847	-0.08
0.30	1.89	-87.7	-73.2	891	-0.38
0.35	2.24	-82.1	-51.3	934	-0.80
0.40	2.24	-78.6	-27.2	975	-1.33
0.45	2.14	-75.1	4.4	1015	-2.00
0.50	2.14	-69.3	56.8	1051	-3.02
0.55	2.36	-58.8	154.4	1081	-4.72
0.60	2.88	-44.5	317.3	1103	-7.21
0.65	3.73	-35.3	502.9	1127	-9.56
0.70	4.87	-40.1	609.3	1165	-10.33
0.75	6.21	-54.4	608.5	1218	-9.35
0.80	7.61	-69.8	547.6	1278	-7.42
0.85	8.87	-82.6	464.6	1340	-5.21
0.90	9.73	-92.3	373.7	1401	-3.09
0.95	9.90	-99.0	277.8	1457	-1.30
1.00	9.00	-103.1	175.9	1509	0.00

4. Conclusion

The deferiprone solubility in the 2-propanol + water mixtures were studied in this work, and their thermodynamic properties were studied according to the Gibbs and van't Hoff equation. The findings demonstrated that the solubility of deferiprone increased as the 2-propanol mass fraction increased up to w_1=0.6 and temperature increased in all mixtures. According to thermodynamic parameters, the dissolution behavior of deferiprone was non-spontaneous, endothermic, and favorable from the point of view of entropy. Additionally, all data generated here were correlated to the mathematical models, and their back-calculated data prove their ability for solubility prediction. The experimental and calculated solubility results in this work would be helpful for the optimization of deferiprone drug preparation, theoretical research, and crystallization and open doors for future research in understanding the solubility behavior and thermodynamic properties of deferiprone, which can have significant implications in the development and optimization of drug formulations and theoretical investigations related to this drug.

Acknowledgments

The Student Research Committee approved and supported the research protocol under grant number 67767, Faculty of Pharmacy, Tabriz University of Medical Sciences, Tabriz, Iran.

Conflict of interest

The authors declare to have no conflict of interest.

References

[1]. R. Vij,R.F. Machado, Pulmonary complications of hemoglobinopathies. Chest, 138 (2010) 973-983.

[2]. N.T. Tran, B. Akkawat, N.P. Morales, P. Rojnuckarin, R. Luechapudiporn, Antiplatelet activity of deferiprone through cyclooxygenase-1 inhibition. Platelets, 31 (2020) 505-512.

[3]. P. Joly, C. Pondarre, C. Badens. Beta-thalassemias: molecular, epidemiological, diagnostical and clinical aspects. in Annales de biologie clinique. 2014.

[4]. A.T. Taher,A.N. Saliba, Iron overload in thalassemia: different organs at different rates. Hematology 2014, the American Society of Hematology Education Program Book, 2017 (2017) 265-271.

[5]. L. Iuliano, F. Violi, J.Z. Pedersen, D. Praticò, G. Rotilio, F. Balsano, Free radical-mediated platelet activation by hemoglobin released from red blood cells. Archives of biochemistry and biophysics, 299 (1992) 220-224.

[6]. I. Panigrahi,S. Agarwal, Thromboembolic complications in β-thalassemia: beyond the horizon. Thrombosis research, 120 (2007) 783-789.

[7]. G.J. Kontoghiorghes, Prospects for introducing deferiprone as potent pharmaceutical antioxidant. Frontiers in Bioscience-Elite, 1 (2009) 161-178.

[8]. M. El Alfy, T.T. Sari, C.L. Lee, F. Tricta, A. El-Beshlawy, The safety, tolerability, and efficacy of a liquid formulation of deferiprone in young children with transfusional iron overload. Journal of pediatric hematology/oncology, 32 (2010) 601-605.

[9]. S. Venkatesh,R.A. Lipper, Role of the development scientist in compound lead selection and optimization. Journal of pharmaceutical sciences, 89 (2000) 145-154.

[10]. C.A. Lipinski, F. Lombardo, B.W. Dominy, P.J. Feeney, Experimental and computational approaches to estimate solubility and permeability in drug discovery and development settings. Advanced drug delivery reviews, 64 (2012) 4-17.

[11]. L. Di, E.H. Kerns, G.T. Carter, Drug-like property concepts in pharmaceutical design. Current pharmaceutical design, 15 (2009) 2184-2194.

[12]. L. Di, P.V. Fish, T. Mano, Bridging solubility between drug discovery and development. Drug discovery today, 17 (2012) 486-495.

[13]. A. Jouyban, Review of the cosolvency models for predicting solubility of drugs in water-cosolvent mixtures. Journal of Pharmacy & Pharmaceutical Sciences, 11 (2008) 32-58.

[14]. M. Abbasi, F. Martinez, A. Jouyban, Prediction of deferiprone solubility in aqueous mixtures of ethylene glycol, propylene glycol and polyethylene glycol 400 at various temperatures. Journal of Molecular Liquids, 197 (2014) 171-175.

[15]. A. Fathi-Azarbayjani, M. Abbasi, J. Vaez-Gharamaleki, A. Jouyban, Measurement and correlation of deferiprone solubility: investigation of solubility parameter and application of van't Hoff equation and Jouyban–Acree model. Journal of Molecular Liquids, 215 (2016) 339-344.

[16]. A. Jouyban, M. Abbasi, E. Rahimpour, M. Barzegar-Jalali, J. Vaez-Gharamaleki, Deferiprone solubility in some non-aqueous mono-solvents at different temperatures: experimental data and thermodynamic modelling. Physics and Chemistry of Liquids, 56 (2018) 619-626.

[17]. C. Zhou, X. Shi, H. Wang, N. An, Measurement and correlation of solubilities of trans-ferulic acid in solvents. JOURNAL OF CHEMICAL INDUSTRY AND ENGINEERING-CHINA-, 58 (2007) 2705.

[18]. H. Buchowski, A. Ksiazczak, S. Pietrzyk, Solvent activity along a saturation line and solubility of hydrogen-bonding solids. The Journal of Physical Chemistry, 84 (1980) 975-979.

[19]. A. Jouyban,W.E. Acree Jr, Mathematical derivation of the Jouyban-Acree model to represent solute solubility data in mixed solvents at various temperatures. Journal of Molecular Liquids, 256 (2018) 541-547.

[20]. A. Jouyban-Gharamaleki, The modified Wilson model and predicting drug solubility in water-cosolvent mixtures. Chemical and pharmaceutical bulletin, 46 (1998) 1058-1061.

[21]. S. Vahdati, A. Shayanfar, J. Hanaee, F. Martínez, W.E. Acree Jr, A. Jouyban, Solubility of carvedilol in ethanol+ propylene glycol mixtures at various temperatures. Industrial & Engineering Chemistry Research, 52 (2013) 16630-16636.

[22]. G.L. Perlovich, S.V. Kurkov, A. Bauer-Brandl, Thermodynamics of solutions: II. Flurbiprofen and diflunisal as models for studying solvation of drug substances. European journal of pharmaceutical sciences, 19 (2003) 423-432.

[23]. Wishart DS, Knox C, Guo AC, Cheng D, Shrivastava S, Tzur D, Gautam B, Hassanali M. DrugBank: a knowledgebase for drugs, drug actions and drug targets. Nucleic Acids Res. 2008 Jan;36(Database issue):D901-6.

[24]. A. Barton, Expanded cohesion parameters. Chapter 5. Handbook of solubility parameters and other cohesion parameters, (1991).

[25]. R.F. Fedors, A method for estimating both the solubility parameters and molar volumes of liquids. Polymer Engineering & Science, 14 (1974) 147-154.

[26]. Y. Marcus, On the preferential solvation of drugs and PAHs in binary solvent mixtures. Journal of Molecular Liquids, 140 (2008) 61-67.

[27]. A. Jouyban, W.E. Acree Jr, F. Martínez, Modeling the solubility and preferential solvation of gallic acid in cosolvent+ water mixtures. Journal of Molecular Liquids, 224 (2016) 502-506.